DOI 10.52209/2706-977X_2026_2_102 IRSTI 81.09.81 UDC 625.84

Modeling of Design Stresses Caused by Vehicular Loading on Cement Concrete Pavement for Conducting Model Tests

Lukpanov R.[1], Kabdyrova L.[1]*, Karacasu M.[2], Yenkebayev S.[3], Tsygulyov D.[1]
[1]Faculty of Architecture and Construction, L.N. Gumilyov Eurasian National University, Astana, Kazakhstan
[2]Eskisehir Technical University, Eskisehir, Turkey
[3]Technobius, LLP, Astana, Kazakhstan
*corresponding author

Abstract: The article presents the results of calculations of stresses caused by tire pressure on the road surface, which are necessary for modeling design situations on a scale. Calculations of actual stresses were performed based on the standard characteristics of tires, the permissible load capacity of motor vehicles, and the potentially variable air pressure in the tire. The latter has a particular influence on the change in the contour area of the contact patch. The calculation of model stresses for the model wheel was performed based on the law of dynamic similarity from the condition of the scale ratio of the actual contact area to the model area, taking into account the elastic properties of the model wheel rubber (determined by laboratory tests). The results of the study are presented as the minimum and maximum values of actual and model stresses by category (types according to main characteristics) of motor vehicles. According to the results, stresses were obtained from the model wheel depending on the type of motor vehicle (described in detail in the article), which range from 0.5 kg/cm² (bicycles) to 12.4 kg/cm² (trucks and buses). The proposed calculation method will allow simulating the calculated stresses from motor vehicle wheels for any model tests on a scale with a high degree of correspondence (to actual stresses).

Keywords: road surface, icing, contact patch, modeling, abrasion.

Introduction

Road construction plays a key role in the development of infrastructure, the economy, and society as a whole. To ensure the sustainable socio-economic development of a country, it is necessary not only to build new roads but also to maintain them in proper condition. The scope of road maintenance work directly depends on the climatic characteristics of the region. In areas with a variable climate, the urgent task is to prevent road surface icing in winter. In modern road construction practice, cement concrete and asphalt concrete pavements are widely used [1]. Concrete roads have a number of undeniable advantages over asphalt concrete roads, including increased durability, high strength, and resistance to frost heaving of the base. However, one of the significant disadvantages of concrete roads is their tendency to ice up at low temperatures, which negatively affects traffic safety during the cold season [2].

The most common method of preventing icing in domestic practice is to treat roads with sand or other abrasive materials, but this approach has its drawbacks, both in terms of effectiveness and appearance [3]. First, the effect of sand is short-lived, especially in heavy traffic. Second, flying sand particles, along with dirt and ice, contaminate vehicles and impair visibility, which increases the likelihood of accidents. Salt or other chemicals (sodium chloride, calcium chloride with or without corrosion inhibitors, potassium acetate, and agricultural products) are also often used worldwide for deicing [4]. Unlike sand, the use of salt has many negative consequences. In addition to the aforementioned disadvantages, such as low efficiency and pollution, salt impairs traction, as melting ice creates a wet road with poor characteristics. When dissolved in water, salt releases active ions through hydrolysis and has a destructive effect on road surfaces and cars, causing corrosion. The issue of chloride concentrations in water after de-icing treatment and their impact on the environment has been actively discussed in the European Parliament since 2006 [5].

The problem of icing on concrete roads remains significant, and its solution may lie in the use of impregnations that do not require regular maintenance but effectively reduce or completely prevent ice formation [6]. In addition to technological characteristics, the economic feasibility of such compositions is becoming an important aspect [7].

The technological solution for preventing icing proposed in the article stands out among existing solutions not only for its design features, but also for its composition, if considered as a hydrophobic agent. The production of the ice-repellent composition is planned to be based on keratin-containing substances obtained from livestock waste, with the addition of water-soluble polymers. In general, the use of polymer components in building materials science is of great importance [8]. In our case, the polymer component acts as a shielding hydrophobic layer. Since concrete is a hydrophilic material that absorbs water, a greater effect will be achieved by using a concentrate of the impregnating composition in water. That is, the water that tends to penetrate the concrete structure will carry with it the suspended mixture of the polymer component of the impregnating composition. This will ensure that the porous surface structure of the concrete is enveloped, creating a layer of tension difference that prevents ice and concrete from becoming a single monolith (as a result, the ice breaks even with minor mechanical impact) [8].

The aim of the general study is to develop an impregnating composition that helps reduce the adhesive resistance of ice crust to concrete roads. However, this article presents part of the study related to the method of calculating and analyzing the design stresses from motor vehicle wheels when modeling design situations on a scale. The results presented may be of interest not so much in terms of the quantitative data obtained, but in terms of the method used to convert real vehicle stresses into model stresses, and the factors and laws that were used for this purpose. Qualitative modeling of design situations, including design loading diagrams, will primarily affect the quality of the results obtained.

To model samples to scale, similarity laws are typically used, which ensure correct comparison of results between the model and the real object [9]. A distinction is made between geometric similarity, which is based on the fact that the model and the real object must have the same geometric shapes but differ in scale [10]. Kinematic similarity is based on the proportionality of velocity, acceleration, and displacement of points in the model and the real object [11]. In dynamic similarity, in order to maintain the equality of forces between the model and the real object, it is necessary to observe the proportionality between all types of forces, and in physical similarity, the materials of the model and the real object must have the same dimensionless parameters characterizing their behavior [12-13]. In our case, the law of dynamic similarity was also used, but the results of the ratios of the forces acting from the wheel load were corrected relative to the contact area values, taking into account the elastic properties of the model wheel rubber, and are described further in the methodology and research results section.

1. Materials and methods

The anti-icing impregnating composition investigated in the broader research project is based on keratin containing agricultural waste and polymer components. Since the present study focuses on stress modeling and scaling procedures, only information relevant to the wear resistance testing program is presented.

The need to recalculate normal stresses on concrete roads caused by motor vehicles was due to model tests of the wear resistance of the impregnating composition. Since the tests were large-scale, high-quality modeling of design situations with adjustments to design schemes and loads was a priority task of the study. The quality of the simulation of the calculation schemes determines the quality of the results of subsequent tests on the wear resistance of the ice-repellent coating, which were performed using equipment designed to assess the abrasion of concrete – an abrasion circle (Figure 1). The tests are large-scale, therefore, the wheel load was calculated using the dynamic similarity method based on the real stress transmitted from the car wheel to the concrete road surface.

In this case, it is not the scale of the actual and model wheels that is important, but the ratio of the contact patch sizes under load, which depends on the tire pressure and the elasticity of the model wheel. However, stresses are directly related to scaling, since their values are a guideline for selecting loads for a scale model wheel (see results, Table 2 - Calculation of normal loads on a model wheel). For this purpose, motor vehicles were conditionally divided into 5 categories according to their load capacity: A1 - bicycles; A2 - motorcycles (mopeds); A3 – passenger cars; A4 - light trucks and buses with particularly low capacity; A5 - trucks and buses.

A – General view of the test

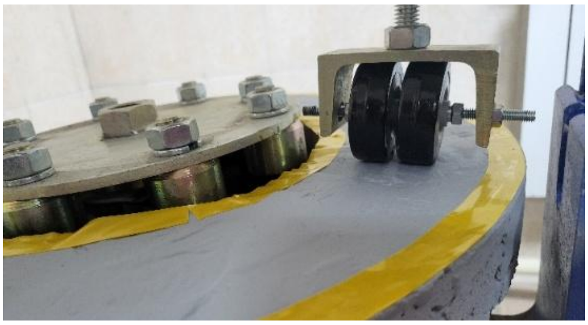

B – Model wheel of a motor vehicle

Fig. 1.- Wear resistance testing of the impregnating composition on an abrasion wheel

The contour area of the contact patch is calculated using the formula for the area of an ellipse [1]. The use of this method is attractive because the parameters of the universal tire characteristic — coefficients c_1 (m²/kN) and c_2 (1/m), determined by calculation from the linear graph of the universal tire characteristic, constructed in the coordinate system (XOY), where x=f/($p_w - p_0$) and y=f²/G_k, together with the coefficient p_0 (kPa), determined by the tire's ply count n, are constant for each tire. They allow the calculation of the normal deflection of the tire, the linear dimensions of the tire tread contact patch—width b_k and length a_k and the contour area of the contact patch on a flat, rigid surface F_k for any combination of normal load on the tire G_k and internal tire air pressure p_w, [1].

$$S_t = \frac{\pi}{4}\frac{20.5}{11.9+\left|\frac{D}{B}-\frac{|n-9|}{2}-3\right|} \times \sqrt{D \times \left(\frac{D}{2}-r_s\right) - \left(\frac{D}{2}-r_s\right)^2} \times 2\sqrt{2 \times \frac{B+(D-d)/2}{2.5} \times \left(\frac{D}{2}-r_s\right) - \left(\frac{D}{2}-r_s\right)^2} \quad (1)$$

Where, S_t - is the contour area of the contact patch, m2; D - is the outer diameter of the tire, m; B - is the width of the tire profile, m; n - is the tire ply ratio; r_s - is the static radius of the tire, m; d - is the nominal rim diameter, m.

The tire characteristics used to determine the contour area of the contact patch for each type of transport were taken from standards and are summarized in Table 1 [15-19].

Table 1. Tire characteristics

Category	Tire width (d), mm	Tire pressure, MPa	Maximum permissible load (F) for single and twin wheels, kN		Linear load F/d, kN/m
			S	D	
A1 (GOST 4750)	28-59	0.19-0.40	0.29-0.85		4.99-21.02
A2 (GOST 5652)	67-180	0.15-0.35	0.98-3.29		11.62-29.88
A3 (GOST 52900)	140-206	0.17-0.21	2.6-5.7		18-56-29-69
A4 (GOST 4754)	154-218	0.20-0.59	4.2-14.2		27.06-62.37
A5 (GOST 5513)	213-425	0.73-0.90	13.34-50.52	12.26-35.80	57.56-125.77

According to the requirements, the pressure deviation from the standard value is within ±2-5%, but in the calculations, a higher value of ±15% was used, which will significantly increase the stress range and will not contradict the real operating conditions of vehicles. When the pressure decreases, the static radius will decrease and the static deflection will increase, therefore the contact patch will increase. Conversely, when the pressure increases, the contact patch will increase, and consequently, the stress transmitted by the wheel will also increase. Thus, voltage range calculations will be performed at maximum (ρ_{max}), standard (ρ_{St}) and minimum (ρ_{min}) tire pressures.

To simulate actual stresses in model tests, the law of dynamic similarity was used based on the scale ratio of the actual contact area to the model area. To determine the model contact area, we will use the results of loading the model wheel rubber with specified loads (see the results section below).

The tests consist of measuring the vertical deformation of the rubber sample under normal compression (Figure 2). The lateral relative deformations were determined under the assumption of constant volume (although, strictly speaking, this condition is not fully satisfied for real rubber materials) and by adopting an average Poisson's ratio for rubber of 0.5. However, since rubber is generally considered a nearly incompressible material with a Poisson's ratio close to 0.5, this assumption is acceptable for engineering estimation of the contact area and the corresponding stresses. To determine the test program (maximum load during testing), preliminary calculations were performed to estimate the expected range of loads acting on the model wheel.

The tests were performed using a certified and calibrated DMA device (Mettler Toledo), which allows a static load to be applied to the sample, followed by measurement of its deformation. The tests were performed at a standard temperature of 22°C and humidity of 50% (constant throughout the entire test period). Vertical deformations were recorded by the device in automatic mode, and horizontal deformations were recorded using a certified and calibrated digital caliper (Sylva System) with a measurement accuracy of 0.01 mm. The loading rate was irrelevant, as the aim of the study was to apply a stepwise load to the rubber sample and then record its volumetric deformation.

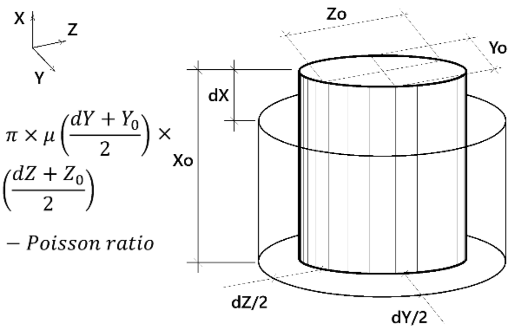

$$S = \pi \times \mu \left(\frac{dY + Y_0}{2}\right) \times$$
$$\times \mu \left(\frac{dZ + Z_0}{2}\right)$$

$\mu - Poisson\ ratio$

DMA testing

Fig. 2.- Testing of a rubber model wheel

2. Results and discussion

As mentioned earlier, tire pressure will have a significant impact on the stress transmitted by the wheel. Based on the previously agreed tire pressure criteria, Figures 3-5 show the results of calculations of stress ranges at maximum (ρ_{max}), standard (ρ_{St}), and minimum (ρ_{min}) tire pressures.

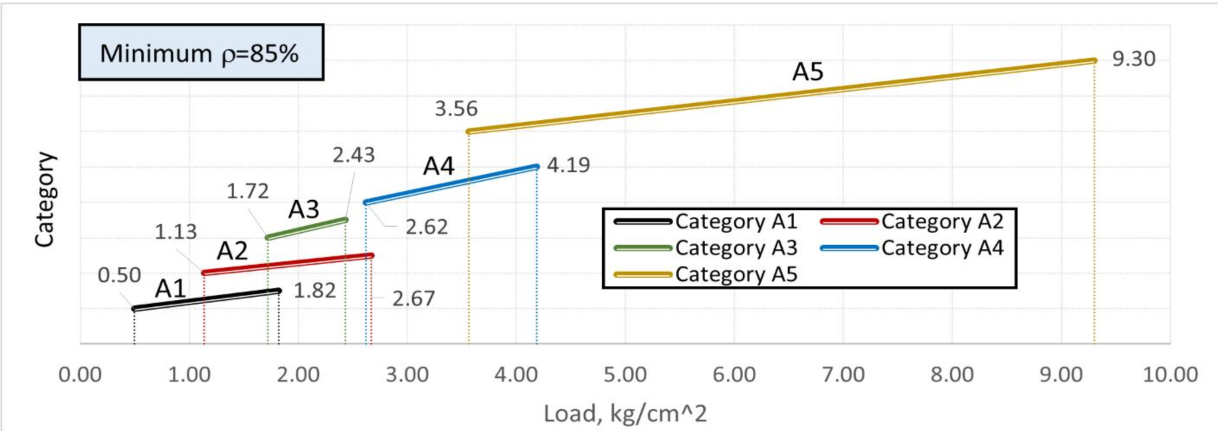

Fig 3. - Voltage range at minimum tire pressure

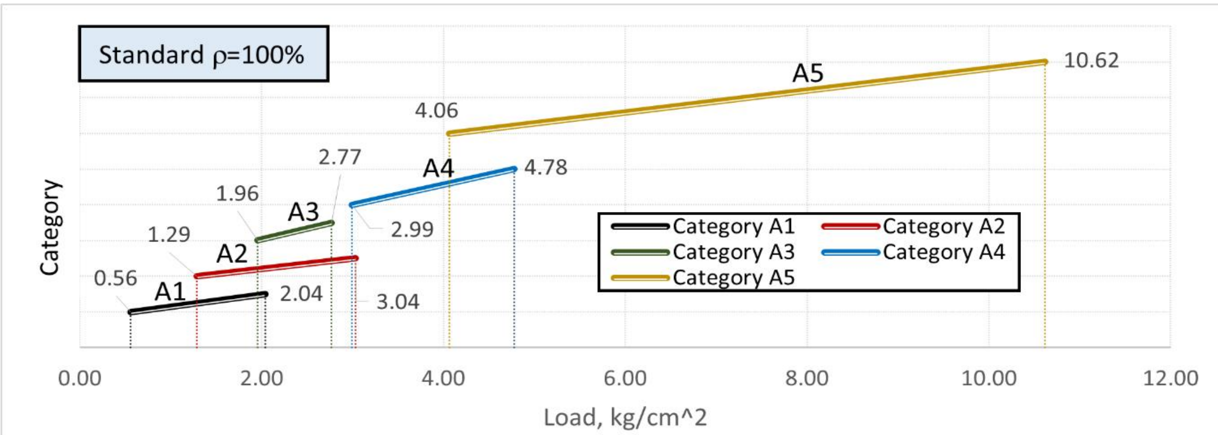

Fig 4. - Voltage range at standard tire pressure

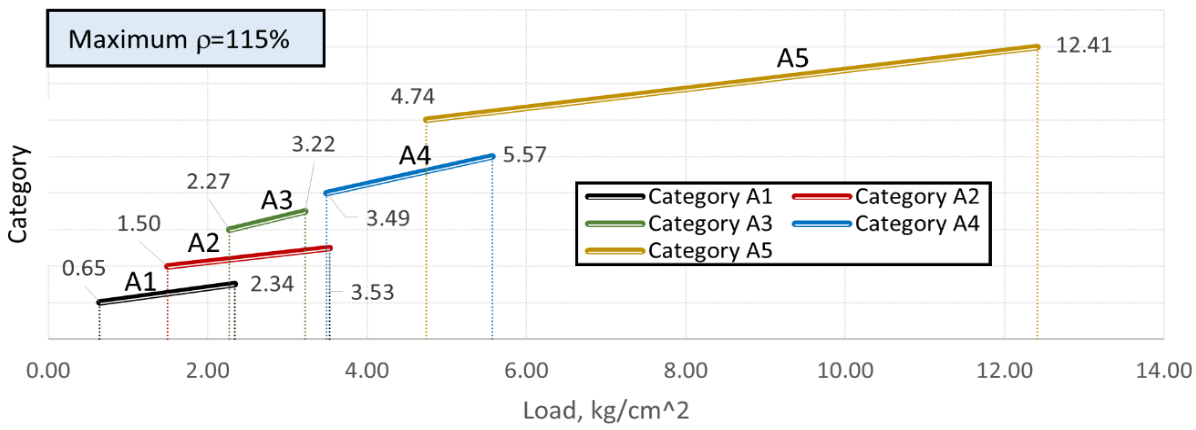

Fig 5. - Voltage range at maximum tire pressure

According to the calculation results for category A1, the decrease in normal stress at minimum tire pressures relative to the standard tire pressure $\left(100 \times \frac{\rho_{min}}{\rho_{st}} - 100\right)$, ranges from -10.8 to 11.3%, while the increase in normal stress at maximum tire pressures relative to the standard tire pressure $\left(100 \times \frac{\rho_{max}}{\rho_{st}} - 100\right)$, ranges from 28.6 to 30.2%. For category A2, the decrease in normal stress is 12.1% (both at maximum and minimum load), and the increase varies from 32.1 to 32.2%. For category A3, the decrease in normal stress varies from 12.0 to 12.2%, and the increase varies from 32.0 to 32.6%. For category A4, the decrease in normal stress is 12.3% (for both cases), and the increase varies from 33.0 to 33.1%. For category A5, the decrease in normal tension varies from 12.3 to 12.4%, and the increase varies from 33.0 to 33.4%. Overall, it was found that the decrease and increase in normal tension for all categories of motor vehicles are very similar, i.e., they do not depend significantly on the load capacity by tire width. Thus, regardless of the category of motor vehicle, it can be concluded that: when tire pressure is reduced by 15% from the standard, the stress from the motor vehicle wheel on the road surface is reduced from the standard stress by 12.0±0.32% (0.32 – confidence interval); when the tire pressure is increased by 15% from the standard, the stress from the wheel increases from the standard by 32.0±0.94% (0.94 – confidence interval).

Figure 6 shows the results of compression tests on model wheel rubber: Figure 6A shows measurements of vertical deformation of the rubber along the X-axis; Figure 6B shows calculations of horizontal deformation along the Y-axis (along the wheel), based on a Poisson's ratio of 0.5; Figure 6C shows the calculations of horizontal deformation along the Z axis (across the wheel), based on a Poisson's ratio of 0.5; Figure 6D shows the calculations of changes in the contact patch contour; Figure 6E shows changes in normal stress from the applied load.

According to the measurement results, the maximum relative deformations at the maximum wheel load of 20 kg were: along the X-axis – 0.14%, along the Y- and Z-axes – 0.07%.

At the same time, attenuation of the deformation processes of the model wheel is observed when the maximum test load is applied, and the deformation values of the penultimate and last stages remain unchanged (at least within the hundredths range). The maximum increase in contact area is 15% of the initial area (without load), which corresponds to the maximum normal stress equal to $\sigma = \frac{20\ \text{kg}}{1.348\ \text{cm}^2} = 14.8\text{kg/cm}^2$. To determine the exact values of the model wheel loads, we will use interpolation based on the previously determined maximum and minimum wheel load values (Figures 3-6).

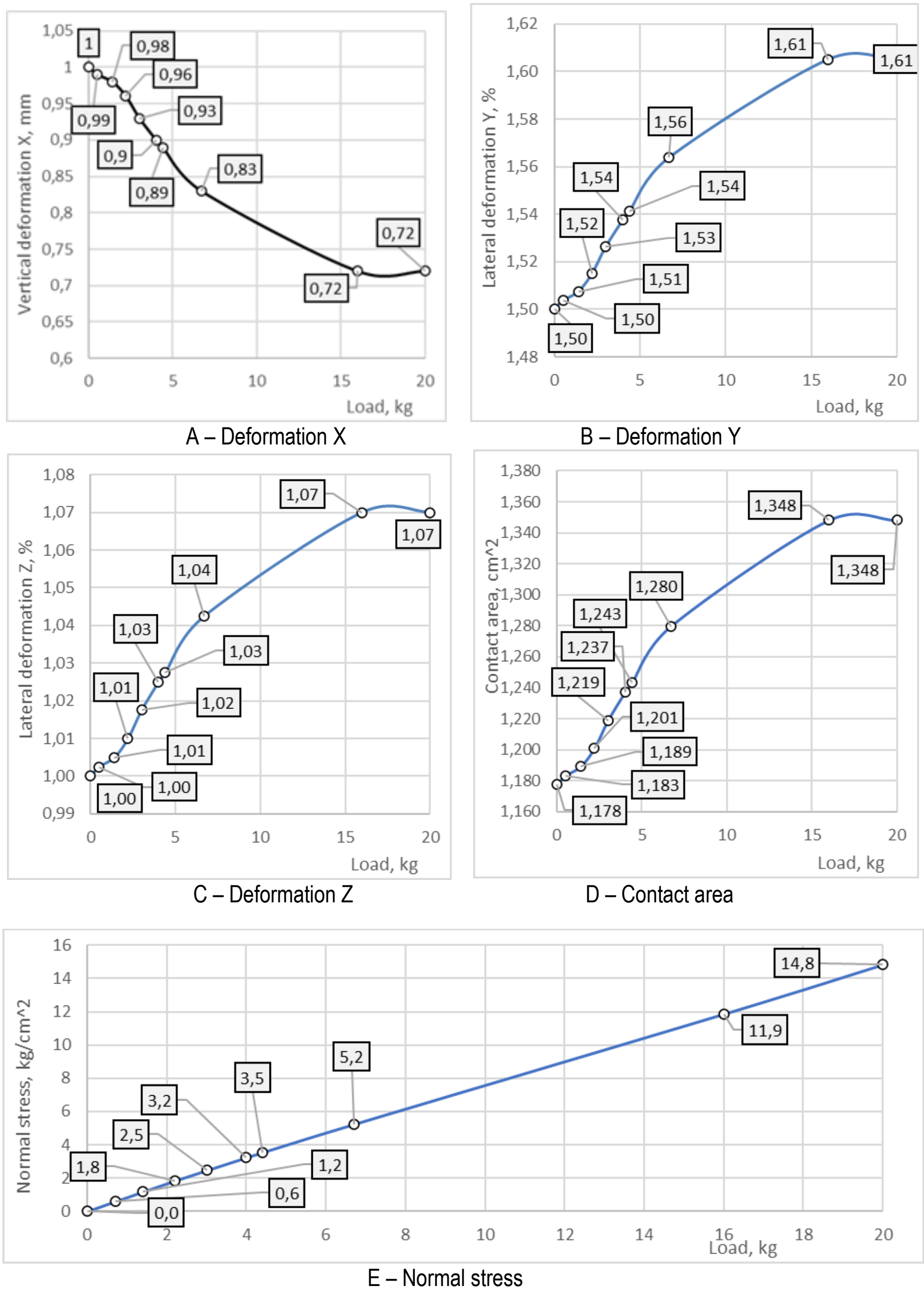

Fig. 6.- Results of compression tests on a model wheel

Table 2 shows the results of calculations of the minimum and maximum normal loads on the model wheel, taking into account the deformation of the model wheel, based on the previously determined stresses of the actual vehicle. As a check, the stresses on the actual wheel correspond to the loads on the model wheel.

Table 2. Calculation of normal loads on a model wheel

Category		Tension of the full-size wheel, kg/cm^2 (Figures 3-5)	Model wheel load, kg (calculated by interpolation of values in Figure 6)	Contact area of the model wheel, cm^2 (calculated by interpolation of the values in Figure 6)	Model wheel tension, kg/cm^2 Check $= \frac{\text{column (3)}}{\text{column (4)}}$
1		2	3	4	5
A1	Min	0.50 (0.049)	0.56 (5.49)	1.13	0.50 (0.049)
	Max	1.13 (0.111)	1.36 (13.34)	1.20	1.13 (0.111)
A2	Min	1.72 (0.169)	1.84 (18.04)	1.07	1.72 (0.169)
	Max	2.62 (0.260)	2.82 (27.65)	1.08	2.62 (0.260)

Continuation of Table 2

1	2	3	4	5	
A3	Min	2.34 (0.230)	2.60 (25.50)	1.11	2.34 (0.230)
	Max	3.56 (0.349)	4.42 (43.35)	1.24	3.56 (0.349)
A4	Min	3.22 (0.317)	3.59 (35.21)	1.11	3.22 (0.317)
	Max	3.53 (0.346)	3.82 (37.46)	1.08	3.53 (0.346)
A5	Min	5.57 (0.546)	5.90 (57.86)	1.06	5.57 (0.546)
	Max	12.40 (1.22)	16.40 (160.83)	1.32	12.40 (1.22)

The results of calculations and measurements will be used for further research into the abrasion resistance of the impregnating composition when simulating the movement of loaded vehicles of different categories. The research results will allow simulating calculated situations taking into account the maximum stress (at maximum tire pressure of vehicles with maximum load capacity values within their category) and minimum stress (at minimum tire pressure for vehicles with minimum load capacity within their category). Thus, we will obtain the maximum and minimum service life of the impregnating composition, taking into account the intensity of use of a particular type of vehicle.

Conclusion

1. Statistical studies of vehicle types were conducted based on key characteristics, followed by their classification into categories, within which they were differentiated according to tire technical characteristics. Within each category of motor vehicles, the standard loads from motor vehicles on the road surface were graded, and the minimum and maximum stresses transmitted by the wheel were determined. At the same time, the maximum and minimum stresses (depending on the standard load capacity and tire contact patch) were further divided into minimum and maximum values depending on the tire pressure (Figures 3-5).

2. The obtained samples (maximum and minimum stress values) were used to calculate the stresses of the model wheel, taking into account the deformation properties of the rubber model wheel. For this purpose, the model wheel was loaded on a press with the vertical deformation of the sample fixed. The calculation results (Figure 6, Table 2) are presented as loads on the model wheel necessary to reproduce the normal stresses of the model wheel on a model road surface identical to the actual one.

3. The proposed method for adjusting wheel loads for large-scale testing allows for more accurate calculation of large-scale design load situations on road surfaces by motor vehicles, taking into account standard loads, corresponding contact patch areas, and the elastic properties of the model wheel. The results obtained have a high degree of reliability, as evidenced by statistical indicators with a confidence interval not exceeding 1.0%.

Acknowledgments

This research was/is funded by the Scientific Committee of the Ministry of Science and Higher Education of the Republic of Kazakhstan (grant No. AR26197579 «Development of the composition and production technology of an anti-icing reagent for concrete roads based on latex emulsion and agricultural waste»).

References

[1] Saleh M., Ahmed N., Moghaddam T. B., & Hashemian L. Towards a high-performance asphalt concrete for extreme climatic conditions using asphaltenes and polyethylene terephthalate fibres //Construction and Building Materials, Vol. 420, 2024, 135573. https://www.sciencedirect.com/science/article/abs/pii/S0950061824007141

[2] Kydyrbay N., Adotey E., Zhazitov M., Suiindik Z., Toktarbay Z., Nuraje N., Toktarbaiuly O. Enhancing road durability and safety: a study on silica-based superhydrophobic coating for cement surfaces in road construction //Engineered Science, Vol. 30, 2024, 1221. https://www.espublisher.com/journals/articledetails/1221/

[3] Lukpanov R. E., Dyussembinov D. S., Yenkebayev S. B., Tsygulyov D.V. Impregnation composition to increase the ice-phobic properties of concrete roads //Retrieved from www.scopus.com, Vol.173, 2022, pp.305-311. https://doi:10.1007/978-3-030-81289-8_39

[4] Mudiyono R., Haidar A. D., Fredy A. Analysis of Environmentally Friendly Concrete (Green Concrete) Using Coal Fly Ash as a Substitute Material for Portland Cement in Road Pavement // IOP Conference Series: Earth and Environmental Science,Vol. 1321, No. 1, 2024, p. 012043. IOP Publishing. https://www.mdpi.com/1996-1944/17/13/3162 https://doi.org/10.21122/2227-1031-2016-15-2-87-94

[5] Pshembaev M. K., Kovalev Ya. N., Yaglov V. N., Girinsky V. V. Methods of combating winter slipperiness //Science and Technology, Vol.19, No.3, 2020, pp.230-240. https://doi:10.21122/2227-1031-2020-19-3-230-240

[6] Lukpanov R. E., Dyussembinov D. S., Yenkebayev S. B., Tsygulyov, D. V. Impregnation composition to increase the ice-phobic properties of concrete roads. Springer International Publishing //Lecture Notes in Civil Engineering Digital Technologies in Construction Engineering, Vol.173, 2022, pp.305-311. https://doi:10.1007/978-3-030-81289-8_39

[7] Ma H., Yang R., Qian S. Research on asphalt concrete pavement deicing technology //Journal of Southeast University (English Edition). Vol.30, No. 3, 2014, pp. 336–342. https://DOI:10.3969/j.issn.1003-7985.2014.03.015

[8] Pshembaev M. K., Kovalev Ya. N., Shevchuk L. I. Stresses in cement-concrete pavement caused by thermal shock //Science and Technology, Vol.15, No.2, 2016, pp.87-94. https://doi.org/10.21122/2227-1031-2016-15-2-87-94

[9] Lukpanov R., Tsygulyov D., Zhantlessova Z., Altynbekova A., Yenkebayev S., & Kozhahmet M. Selection of equivalent material for soil testing using piles on a scale model testing apparatus //Geomate Journal. Vol. 26, No.117, 2024, Pp.11-18. https://geomatejournal.com/geomate/article/view/4167
[10]Vorobiev V. S., & Apfelbaum E. M. Generalized similarity laws based on some consequences of the Van der Waals equation. //High Temperature Thermophysics, Vol. 54, No.2, 2016, pp. 186-196. https://doi.org/10.7868/S0040364416020253
[11] Loginova M. E., Movsumzade E. M., Fattakhov M. M., Akhtyamov E. K., & Chetvertnev S. S. Development of similarity theories for physicochemical processes. History and pedagogy of natural sciences. No.4, 2022, Pp. 39-42. https://doi.org/10.24412/2226-2296-2022-4-39-42
[12] Barabanov E. A. Kinematic similarity of linear differential systems with a multiplier parameter at the derivative. Journal of Mathematical Sciences //Proceedings of the IG Petrovsky Seminar. Vol. 210, 2015, Pp. 135-147. https://doi.org/10.1007/s10958-015-2552-9
[13]Lukpanov R. E., Yenkebayeva A. S., Tsygulyov D. V., Sabitov Y. Y., & Dyussembinov D. S. Assessment of ash-storage coolector stability using geosynthetic reinforcement elements by tray testing and numerical modeling //News of the National Academy of Sciences of the Republic of Kazakhstan. Series of Geology and Technical Sciences, Vol.3, No.453, 2022, pp. 212-225. https://doi:10.32014/2022.2518-170X.191
[14] Interstate standard GOST 5652 - Pneumatic tires for motorcycles, motorcycles, scooters and mopeds. Technical specifications. 2023, pp. 1-16. https://internet-law.ru/gosts/gost/11351/
[15] Interstate standard GOST 52900 - Pneumatic tires for passenger cars and trailers. Technical specifications. 2023, pp. 1-23. https://internet-law.ru/gosts/gost/47531/
[16] Interstate standard GOST 4754 - Pneumatic tires for passenger cars, trailers, light trucks and buses of small capacity. Technical specifications. 2023, pp. 1-33. https://internet-law.ru/gosts/gost/7152
[17] Interstate standard GOST 5513 - Pneumatic tires for trucks, trailers, buses and trolleybuses. Technical specifications. 2023, pp. 1-22. https://internet-law.ru/gosts/gost/46320/
[18] Interstate standard GOST 4750 - Pneumatic tires for bicycles. Technical specifications. 2023, pp. 1-14. https://internet-law.ru/gosts/gost/11205/

Information of the authors

Lukpanov Rauan Ermagambetovich, PhD, professor, L.N. Gumilyov Eurasian National University
e-mail: rauan_82@mail.ru

Kabdyrova Lyailya Temirzhanovna, Doctoral student at L.N.Gumilyov Eurasian National University
leila_0781@mail.ru

Karacasu Murat, PhD, professor, Eskisehir Technical University
muratk@ogu.edu.tr

Yenkebayev Serik Beisengalievich, PhD., associate professor, Technobius LLP
Yenkebayev-serik@mail.ru

Tsygulyov Denis Vladimirovich, Candidate of Technical Sciences, associate professor, L.N. Gumilyov Eurasian National University, denis_72@mail.ru